Journal of the Optical Society of Korea
Vol. 19, No. 3, June 2015, pp. 297-302

ISSN: 1226-4776(Print) / ISSN: 2093-6885(Online)
DOI: http://dx.doi.org/10.3807/JOSK.2015.19.3.297

Investigation of Terahertz Generation from Bulk and Periodically Poled $LiTaO_3$ Crystal with a Cherenkov Phase Matching Scheme

Zhongyang Li[1]*, Pibin Bing[1], Sheng Yuan[1], Degang Xu[2], and Jianquan Yao[2]

[1]North China University of Water Resources and Electric Power, 36, Bei-huan Road, Zhengzhou, Henan 450045, P. R. China
[2]College of Precision Instrument and Opto-electronics Engineering, Institute of Laser and Opto-electronics, Tianjin University, Tianjin 300072, P. R. China

(Received January 27, 2015 : revised April 9, 2015 : accepted April 10, 2015)

Terahertz (THz) wave generation from bulk and periodically poled $LiTaO_3$ (PPLT) with a Cherenkov phase matching scheme is numerically investigated. It is shown that by using the crystal birefringence of bulk $LiTaO_3$ and a grating vector of PPLT, THz waves can be efficiently generated by difference frequency generation (DFG) with a Cherenkov phase matching scheme. The frequency tuning characteristics of the THz wave via varying wavelength of difference frequency waves, phase matching angle, poling period of PPLT and working temperature are theoretically analyzed. The parametric gain coefficient in the low-loss limit and the absorption coefficient of the THz wave during the DFG process in the vicinity of polariton resonances are numerically analyzed. A THz wave can be efficiently generated by utilizing the giant second order nonlinearities of $LiTaO_3$ in the vicinity of polariton resonances.

Keywords : Terahertz wave, Difference frequency generation, Cherenkov phase matching
OCIS codes : (190.4410) Nonlinear optics, parametric process; (140.3070) Infrared and far-infrared lasers

I. INTRODUCTION

In the study of modern terahertz (THz) optoelectronics, monochromatic THz sources play an important role in high resolution THz applications, such as environmental gas monitoring and high-density and high-speed wireless communications [1-4]. Difference frequency generation (DFG) with two closely spaced laser frequencies ω_1 and ω_2 in second-order nonlinear optics crystals is one of the promising processes for efficient monochromatic THz wave output in the wide frequency tuning range and for room temperature operation [5, 6]. Recently, high-efficiency THz wave generation based on DFG employing Cherenkov phase matching has been intensively researched [7-9]. THz wave generation with Cherenkov phase matching is an attractive scheme because strong THz absorption originated from lattice vibration modes of the nonlinear optical crystal can be overcome. Unfortunately, the maximum frequencies generated by DFG with a Cherenkov phase matching scheme are limited to 7.2 THz [10]. Moreover, the output power of the THz wave within the high-frequency band is extremely low. Such limitations on output frequencies and power are caused by the dramatically increased absorption of the nonlinear materials in the vicinity of polariton resonances. However, at the same time, polariton resonances can induce giant second order nonlinearities [11-13]. The giant second order nonlinearities in the vicinity of polariton resonances can be exploited to extend the output frequencies and enhance the output power of the THz wave. In this paper, we explore THz wave generation based on DFG in the vicinity of polariton resonances with a Cherenkov phase matching scheme. A surface-emitted configuration is employed to overcome the strong absorption problem in the vicinity of polariton resonances. The nonlinear crystals utilized in this paper are bulk and periodically poled $LiTaO_3$ (PPLT). To the best of our knowledge, THz wave generation based on DFG utilizing bulk $LiTaO_3$ and PPLT with a Cherenkov phase matching scheme has not been investigated. The advantage of utilizing $LiTaO_3$ over $LiNbO_3$ lies in the fact that $LiTaO_3$ has a significantly reduced rate of optically-induced index change damage due to the photorefractive effect [14]. According to Ref. [14], the optically induced

*Corresponding author: thzwave@163.com
Color versions of one or more of the figures in this paper are available online.

index-change damage increases at rates of 2.8×10^{-3} $cm^2/\mu W$ and 4.9×10^{-4} $cm^2/\mu W$ in $LiNbO_3$ and $LiTaO_3$, respectively. The second advantage is that the poling electric field required for $LiTaO_3$ is one order of magnitude lower than that for $LiNbO_3$ [15]. The coercive fields are 1.7 kV/mm and 21 kV/mm for stoichiometric $LiTaO_3$ and congruent $LiNbO_3$, respectively [15]. In this paper, a Cherenkov phase matching scheme is realized by using the crystal birefringence of bulk $LiTaO_3$ and a grating vector of PPLT. We numerically simulate the frequency tuning characteristics via varying pump wavelengths, phase matching angle, poling period of PPLT and working temperature. Parametric gain coefficient in the low-loss limit of the THz wave during the DFG process in the vicinity of polariton resonances is numerically analyzed.

II. THEORETICAL MODEL

The schematic drawing of surface-emitted DFG in bulk $LiTaO_3$ and PPLT is presented in Fig. 1. As shown in Fig. 1(a), two input optical waves, λ_1 and λ_2, at the frequencies of ω_1 and ω_2 in the infrared (IR) domain are propagating collinearly along the X axis in a bulk $LiTaO_3$ crystal and are polarized along the Z and Y axes, respectively. The two optical waves are located close to the lateral surface (XY) of the crystal. A THz wave is emitted due to the oscillating nonlinear polarization at the difference frequency between the two input waves. The radiation angle α between directions of the optical and THz wave propagation is determined by the refractive index of input optical waves in the crystal, and the refractive index of the THz wave,

$$\cos\alpha = \frac{K_{IR}}{K_{THz}} \tag{1}$$

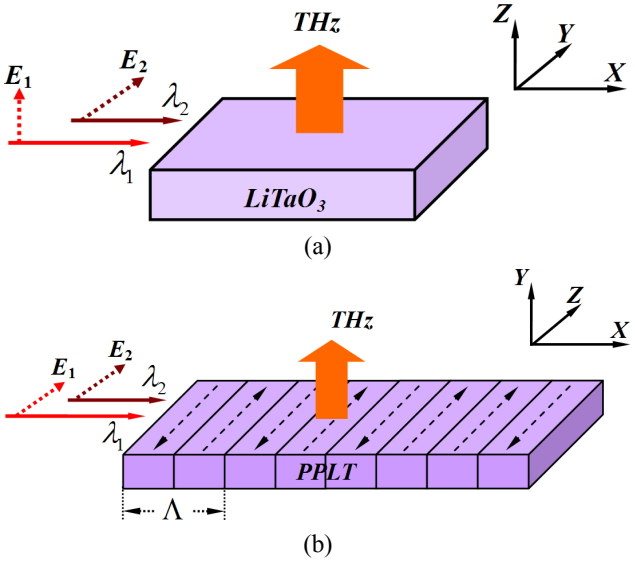

FIG. 1. Schematic diagram of the surface-emitted DFG with a Cherenkov phase matching scheme. (a) $LiTaO_3$, (b) PPLT.

where $K_{THz} = \omega_{THz} n_{THz}/c$ is the wave vector, n_{THz} is the refractive index at ω_{THz} frequency; $K_{IR} = n_1^e(\theta)\omega_1/c - n_2^o\omega_2/c$, $n_1^e(\theta)$ and n_2^o are the extraordinary and ordinary refractive indices of optical waves λ_1 and λ_2 at ω_1 and ω_2 frequencies, respectively. θ is the angle between the directions of the optical wave propagation and the optical axis of $LiTaO_3$. For the THz wave generation based on DFG, the energy conservation condition has to be fulfilled

$$\frac{1}{\lambda_1} = \frac{1}{\lambda_2} + \frac{1}{\lambda_{THz}} \tag{2}$$

where λ_{THz} is the wavelength of the THz wave. From Eq. (1), it follows that the THz wave is emitted perpendicular to the directions of the optical wave propagation if K_{IR}=0. The effective nonlinear coefficient d_{eff} in the DFG process is given by

$$d_{eff} = d_{15}\sin\theta - d_{22}\cos\theta\sin 3\varphi \tag{3}$$

where d_{15} and d_{22} are the nonlinear coefficients, the angle φ is an azimuthal angle of the optical wave vector with respect to the X-axis.

As shown in Fig. 1(b), two input optical waves, λ_1 and λ_2, at the frequencies of ω_1 and ω_2 in the infrared (IR) domain are propagating collinearly along the X axis in the PPLT crystal. Both λ_1 and λ_2 are polarized along the Z axis. The two optical waves are located close to the lateral surface (XZ) of the crystal. The optical axis of the $LiTaO_3$ crystal parallels the Z axis. A THz wave can be generated in a direction perpendicular to the optical wave propagation if poling period Λ of the PPLT satisfies

$$\Lambda = \frac{2\pi}{K_{IR}} \tag{4}$$

The parametric gain coefficient g_0 in the low-loss limit during DFG processes in cgs units can be determined by the following expression [16]:

$$g_0^2 = \frac{\pi\omega_{THz}\omega_2}{2c^3 n_1^e(\theta) n_2^o n_{THz}} I_{\lambda 1}\left(d_E' + \sum_j \frac{S_j\omega_{0j}^2 d_{Qj}'}{\omega_{0j}^2 - \omega_{THz}^2}\right)^2 \tag{5}$$

$$\alpha_{THz} = 2\frac{\omega_{THz}}{c}\mathrm{Im}\left(\varepsilon_\infty + \sum_j \frac{S_j\omega_{0j}^2}{\omega_{0j}^2 - \omega_{THz}^2 - i\omega_{THz}\Gamma_j}\right)^{\frac{1}{2}} \tag{6}$$

where ω_{THz} is the absorption coefficient in the THz region, ω_{0j}, S_j and Γ_j denote eigenfrequency, oscillator strength of the polariton modes and the bandwidth of the jth A_1-symmetry phonon mode in the $LiTaO_3$ crystal, respectively. $I_{\lambda 1}$ is the power density of the optical wave λ_1. d_E' and d_Q' are

nonlinear coefficients related to pure parametric (second-order) and Raman (third-order) scattering processes, respectively. In this letter, the data for $LiTaO_3$ is taken from reference [17].

The theoretical values of the optical wavelengths are calculated using a wavelength- and temperature-independent Sellmeier equation for 0.5% MgO-doped stoichiometric $LiTaO_3$ (MgO: $LiTaO_3$)in the IR [18]. The Sellmeier equation for MgO:$LiTaO_3$ of Dolev et al. [18] in the IR range in a temperature range from room temperature to 200℃ can be written as

$$n_e^2 = a_{1e} + b_{1e}f + \frac{a_{2e}+b_{2e}f}{\lambda^2-(a_{3e}+b_{3e}f)^2} + \frac{a_{4e}+b_{4e}f}{\lambda^2-(a_{5e}+b_{5e}f)^2} - a_{6e}\lambda^2 \quad (7)$$

$$n_o^2 = a_{1o} + b_{1o}f + \frac{a_{2o}+b_{2o}f}{\lambda^2-(a_{3o}+b_{3o}f)^2} + \frac{a_{4o}+b_{4o}f}{\lambda^2-(a_{5o}+b_{5o}f)^2} - a_{6o}\lambda^2 \quad (8)$$

where $a_{1e}=4.5615$, $a_{2e}=0.08488$, $a_{3e}=0.1927$, $a_{4e}=5.5832$, $a_{5e}=8.3067$, $a_{6e}=0.021696$, $b_{1e}=4.782\times10^{-7}$, $b_{2e}=3.0913\times10^{-8}$, $b_{3e}=2.7326\times10^{-8}$, $b_{4e}=1.4837\times10^{-5}$, $b_{5e}=1.3647\times10^{-7}$, $a_{1o}=4.5082$, $a_{2o}=0.084888$, $a_{3o}=0.19552$, $a_{4o}=1.1570$, $a_{5o}=8.2517$, $a_{6o}=0.0237$, $b_{1o}=2.0704\times10^{-8}$, $b_{2o}=1.4449\times10^{-8}$, $b_{3o}=1.5978\times10^{-8}$, $b_{4o}=4.7686\times10^{-6}$, $b_{5o}=1.1127\times10^{-5}$ and $f=(T-24.5)\times(T+570.82)$, T is the crystal temperature in ℃. All the figures in this work were numerically simulated according to the Eqs (1-8) using MATLAB software.

III. FREQUENCY TUNING CHARACTERISTICS

3.1. THz Wave Generation with Bulk $LiTaO_3$

DFG processes are more versatile because of their wide tuning properties. According to Eq. (1-2), the frequencies of the THz wave can be tuned by varying phase-matching angle θ, wavelength of optical waves λ_1 and λ_2 and working temperature T. Figure 2 shows the tuning characteristics versus optical wavelength λ_1. From the figure we find that as λ_1 changes from 0.5 to 3 μm, a THz wave with frequency varying from 0.68 to 0.027 THz can be attained. The frequency of the THz wave is insensitive to the wavelength λ_1 because the refractive index difference between $n_1^e(\theta)$ of optical wave λ_1 and n_2^o of optical wave λ_2 changes relatively little with optical wavelength in the infrared range.

The frequency tuning can be realized by using the dependence of crystal birefringence on angle θ between the directions of the optical wave propagation and optical axis. Figure 3 shows the tuning characteristics versus angle θ. From the figure we find that as θ changes from 0° to 90°, THz wave frequency varying from 0 to 0.3 THz can be attained. The frequency of the THz wave is insensitive to angle θ. As θ changes from 0° to 90°, the effective nonlinear coefficient d_{eff} gradually increases. When θ equals 90°, the d_{eff} reaches the maximum value.

Figure 4 shows the tuning characteristics versus working

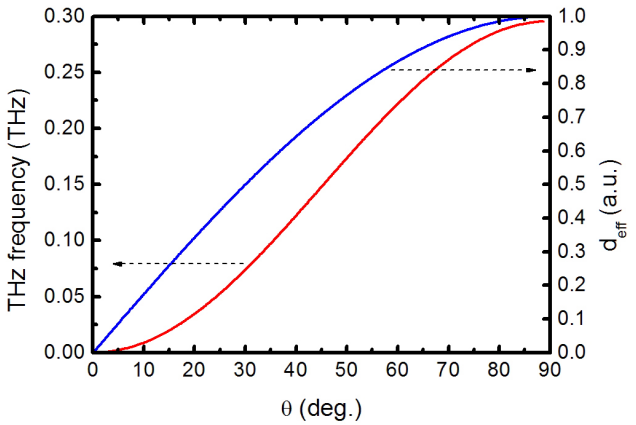

FIG. 3. THz wave frequency versus the angle θ. T=23℃, α = 90°, λ_1=1.064 μm.

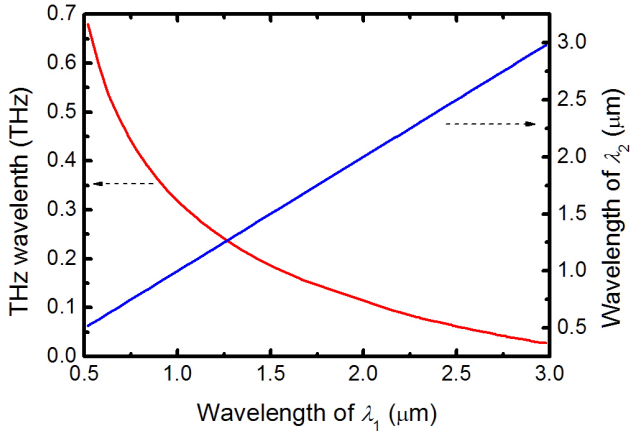

FIG. 2. THz wave frequency versus the wavelength of optical wave λ_1. T=23℃, α = 90°, θ = 90°.

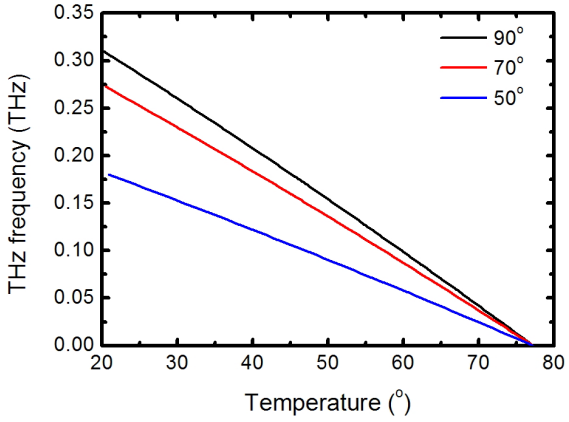

FIG. 4. THz wave frequency versus working temperature T. λ_1=1.064 μm, α = 90°.

temperature T. As working temperature T varies from 20°C to 77°C, THz wave frequency changes are relatively small. The tuning range is relatively limited because the difference between $n_1^e(\theta)$ of optical wave λ_1 and n_2^o of optical wave λ_2 in the infrared range changes relatively little with working temperature T. According to Eq. (6), with the increase of working temperature T the absorption coefficient α_{THz} intensively increases due to the increase of the linewidth Γ_j of the A_1-symmetry phonon modes.

3.2. THz Wave Generation with PPLT

According to Eq. (4), the frequencies of the THz wave can be tuned by varying poling period Λ, wavelength of optical wave λ_1 and λ_2, and working temperature T. Figure 5 shows the tuning characteristics versus optical wavelength λ_1 when the poling period Λ equals 13 μm. From the figure we find that as λ_1 changes from 0.4 to 3 μm, frequencies of the THz wave varying from 8.5 to 10.7 THz can be attained. The frequency of the THz wave can be rapidly tuned by varying the wavelength λ_1 when the wavelength λ_1 is less than 1μm. Different from THz wave generation with bulk $LiTaO_3$ where the frequencies of the generated THz wave are under 1 THz, the frequencies of THz wave generated from PPLT approach the polariton resonances of the $LiTaO_3$ crystal.

As λ_1 equals to 1.064 μm, the frequencies of THz wave versus the poling period Λ of PPLT are depicted in Fig. 6. From the figure we find that as Λ varies from 5 to 60 μm, a THz wave covering a tuning of 2.3 to 27.6 THz can be realized. The tuning range can cover the entire polariton resonances of the $LiTaO_3$ crystal. The frequency of THz wave can be rapidly tuned by varying the poling period Λ for Λ less than 20 μm.

Figure 7 shows the tuning characteristics versus working temperature T. As working temperature T varies from 20°C to 200°C, THz wave frequency changes relatively little. The rapid tuning of a THz wave cannot be realized by varying working temperature.

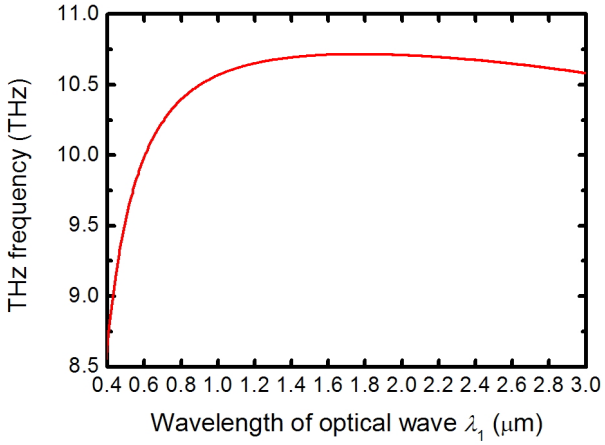

FIG. 5. THz wave frequency versus the wavelength of optical wave λ_1. T = 25℃, Λ=13 μm.

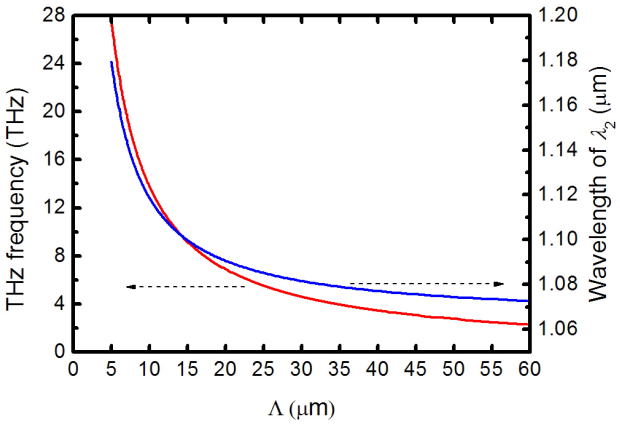

FIG. 6. THz wave frequency versus the poling period Λ of PPLT. T = 25℃, λ_1=1.064 μm.

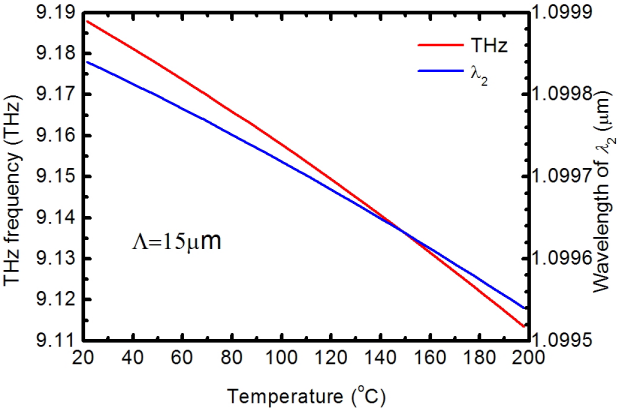

FIG. 7. THz wave frequency versus working temperature T. λ_1=1.064 μm, Λ=15 μm.

IV. PARAMETRIC GAIN CHARACTERISTICS

$LiTaO_3$ crystal has five infrared- and Raman-active transverse optical (TO) phonon modes at the frequencies of 200 cm^{-1}, 241 cm^{-1}, 357 cm^{-1}, 596 cm^{-1}, 657 cm^{-1}, which are called A_1-symmetry modes. The five phonon modes which correspond to the THz wave frequencies of 6 THz, 7.23 THz, 10.71 THz, 17.88 THz and 19.71 THz, are useful for efficient THz wave generation because of the largest parametric gain in the vicinity of phonon polariton resonances, as shown in Fig. 8. From the figure we find that as the THz wave approaches polariton resonances, the parametric gain coefficient g_0 reaches sharply a maximum value and the absorption coefficient α_{THz} increases intensively to a great value. Such dramatic enhancements of parametric gain coefficients can be exploited for improving the output powers and extending the frequency bands of THz waves if a surface-emitted configuration is employed to minimize the propagation path of the THz wave within the crystal.

Compared with other works in which THz wave generations are far from polariton resonances to avoid intensive absorption,

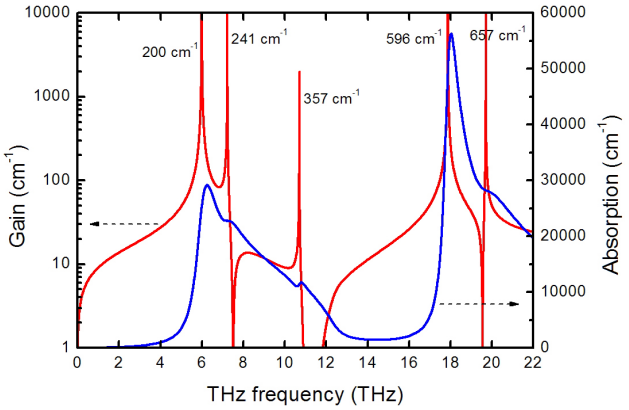

FIG. 8. Parametric gain coefficient in the low-loss limit g_0 and absorption coefficient α_{THz} versus THz wave frequency at room temperature. $\lambda_1 = 1.064$ μm, $I_{\lambda 1} = 200$ MW/cm^2.

the theoretical model proposed in this letter can exploit dramatic enhancement of parametric gain in the vicinity of polariton resonances with a surface-emitted configuration. The theoretical model proposed in this letter is useful to other materials with crystal birefringence properties, such as $LiNbO_3$, KTA, in which polaritons are both infrared-active and Raman-active. The theoretical model is also useful to semiconductor optical waveguides with modal birefringence properties. By utilizing modal birefringence of fundamental TE and TM modes in a planar waveguide, the absorption at polariton resonances can be efficiently reduced [19].

V. CONCLUSION

THz wave generation at polariton resonance of $LiTaO_3$ by DFG processes is investigated. It is shown that by using crystal birefringence of bulk $LiTaO_3$ and grating vector of PPLT, a THz wave can be efficiently generated by DFG in the vicinity of polariton resonances with a Cherenkov phase matching scheme. In the case of bulk $LiTaO_3$, the frequency of the THz wave is insensitive to the wavelength λ_1, phase matching angle and working temperature. In the case of PPLT, the tuning range of a THz wave is widened by varying the poling period Λ. Dramatic enhancement of parametric gain coefficients in the vicinity of polariton resonances can be exploited for improving the output power and extending the frequency bands of a THz wave by using a surface-emitted configuration to minimize the propagation path of a THz wave within the crystal.

ACKNOWLEDGMENT

This work was supported by the National Natural Science Foundation of China (Grant Nos. 61201101, 61205003 and 61172010).

REFERENCES

1. L. Ho, M. Pepper, and P. Taday, "Terahertz spectroscopy: Signatures and fingerprints," Nat. Photon. **2**, 541-543 (2008).
2. Y. Kim, K. H. Jin, J. C. Ye, J. Ahn, and D. Yee, "Wavelet power spectrum estimation for high-resolution terahertz time-domain spectroscopy," J. Opt. Soc. Korea **15**, 103-108 (2011).
3. J. L. Liu, J. M. Dai, S. L. Chin, and X. C. Zhang, "Broadband terahertz wave remote sensing using coherent manipulation of fluorescence from asymmetrically ionized gases," Nat. Photonics **4**, 627-631 (2010).
4. T. Kleine-Ostmann and T. Nagatsuma, "A review on terahertz communications research," J. Infrared Millim. Te. Waves **32**, 143-171 (2011).
5. W. Shi and Y. J. Ding, "A monochromatic and high-power THz source tunable in the ranges of 2.7-38.4 um and 58.2-3540 um for variety of potential applications," Appl. Phys. Lett. **84**, 1635-1637 (2004).
6. P. Zhao, S. Ragam, Y. J. Ding, I. B. Zotova, X. Mu, H. Lee, S. K. Meissner, and H. Meissner, "Singly resonant optical parametric oscillator based on adhesive-free-bonded periodically inverted $KTiOPO_4$ plates: terahertz generation by mixing a pair of idler waves," Opt. Lett. **37**, 1283-1285 (2012).
7. K. Suizu, T. Tsutsui, T. Shibuya, T. Akiba, and K. Kawase, "Cherenkov phase matched THz-wave generation with surfing configuration for bulk lithium nobate crystal," Opt. Express **17**, 7102-7109 (2009).
8. K. Takeya, K. Suizu, and K. Kawase, "THz generation using Cherenkov phase matching," Terahertz Science and Technology **5**, 78-86 (2012).
9. T. Akiba, Y. Akimoto, K. Suizu, K. Miyamoto, and T. Omatsu, "Evaluation of polarized terahertz waves generated by Cherenkov phase matching," Appl. Opt. **53**, 1518-1522 (2014).
10. K. Suizu, T. Akiba, N. Kaneko, H. Uchida, K. Miyamoto, and T. Omatsu, "Cherenkov phase-matched terahertz wave generation and its spectroscopic applications," Proc. SPIE **8909**, 890910 (2013).
11. Y. J. Ding, "Efficient generation of high-frequency terahertz waves from highly lossy second-order nonlinear medium at polariton resonance under transverse-pumping geometry," Opt. Lett. **35**, 262-264 (2010).
12. Y. H. Avetisyan, "Terahertz-wave surface-emitted difference-frequency generation without quasi-phase-matching technique," Opt. Lett. **35**, 2508-2510 (2010).
13. R. Chen, G. Sun, G. Xu, Y. J. Ding, and I. B. Zotova, "Generation of high-frequency terahertz waves in periodically poled $LiNbO_3$ based on backward parametric interaction," Appl. Phys. Lett. **101**, 111101 (2012).
14. O. Eknoyan, H. F. Taylor, W. Matous, T. Ottinger, and R. R. Neugaonkar, "Comparison of photorefractive damage effects in $LiNbO_3$, $LiTaO_3$, and $Ba_{1-x}Sr_xTi_yNb_{2-y}O_6$ optical waveguides at 488 nm wavelength," Appl. Phys. Lett. **71**, 3051-3053 (1997).
15. D. N. Nikogosyan, *Nonlinear Optical Crystals: A Complete Survey* (Springer, New York, USA, 2005).
16. S. S. Sussman, "Tunable light scattering from transverse optical modes in lithium niobate," Report of Microwave Lab, Stanford University, No. 1851, 22-34 (1970).

17. A. S. Barker, Jr., A. A. Ballman, and J. A. Ditzenberger, "Infrared study of the lattice vibrations in $LiTaO_3$," Phys. Rev. B **2**, 4233-4239 (1970).
18. I. Dolev, A. Ganany-Padowicz, O. Gayer, A. Arie, J. Mangin, and G. Gadret, "Linera and nonlinear optical properities of MgO:$LiTaO_3$," Appl. Phys. B **96**, 423-432 (2009).
19. K. Saito, T. Tanabe, and Y. Oyama, "Widely tunable surface-emitted monochromatic terahertz-wave generation beyond the Reststrahlen band," Opt. Commun. **335**, 99-101 (2015).